Electrochemistry Communications 180 (2025) 108050

Contents lists available at ScienceDirect

Electrochemistry Communications

journal homepage: www.elsevier.com/locate/elecom

Modification of platinum surfaces with cerium species for promoting oxidative desorption of adsorbed sulfur

Tetsuro Morooka [a], Tamao Shishido [a], Takuya Nakanishi [a], Takuya Masuda [a,b,*]

[a] Research Center for Energy and Environmental Materials (GREEN), National Institute for Materials Science (NIMS), Tsukuba, Ibaraki 305-0044, Japan
[b] Graduate School of Chemical Sciences and Engineering, Hokkaido University, Sapporo, Hokkaido 060-0810, Japan

ARTICLE INFO

Keywords:
Polymer electrolyte membrane fuel cells (PEMFCs)
Electrocatalysts
Platinum
Single crystal surfaces
Sulfur poisoning

ABSTRACT

Adsorption of sulfur (S) significantly reduces the electrochemically active surface area of platinum (Pt) electrocatalysts in polymer electrolyte membrane fuel cells (PEMFCs), namely, S poisoning. Mitigation techniques against S poisoning are strongly desired for highly durable PEMFCs. A Pt single-crystal surface was demonstrated to be modified with cerium (Ce) species by being immersed in a Ce-containing aqueous solution with hydrogen (H_2) gas bubbling or potential holding at −0.2 V vs. Ag/AgCl. For a Ce-free Pt electrode, electrochemical responses characteristic of the adsorption/desorption of hydrogen and hydroxyl species at the bare Pt surface disappeared due to the adsorbed elemental sulfur, S_{ad}, while the oxidative desorption of S_{ad} from the Pt electrode occurred at around 0.80 V vs. Ag/AgCl. In contrast, for the Ce-modified Pt electrode, the oxidative desorption of S_{ad} occurred at a potential around 0.3 V which is less positive (more negative) than that of Ce-free Pt electrode, showing the enhanced oxidative desorption capability due to the presence of Ce species on the surface. While the Ce species was desorbed from the Pt electrode simultaneously with the oxidative desorption of S_{ad}, the Pt surface can be re-modified with the Ce species by H_2 gas bubbling or potential holding at −0.2 V vs. Ag/AgCl, which is a similar condition to that of anode of PEMFC under operations. Thus, the Ce-modification of Pt surfaces potentially acts as a practical mitigation measure against the S poisoning.

1. Introduction

The activity of electrocatalysts has been enhanced through various technologies [1–4], but promoting the desorption of sulfur (S) species from platinum (Pt) surfaces remains one of the key challenges in polymer electrolyte membrane fuel cells (PEMFCs): PEMFCs, emitting water as the only chemical byproduct and therefore attracting a great deal of attention as clean power sources [5], oxidize hydrogen (H_2) fuel gas to protons in the anode and reduce oxygen from the air to water in the cathode, while the adsorption of pollutants and impurities present in air and fuel gas on the surfaces of Pt catalyst severely degrades the performance of PEMFCs [6–11]. Since strong adsorption of S species significantly inhibits the electrochemical reactions, that is S poisoning [12,13], the mitigation technique against S poisoning is strongly desired for the long-lived PEMFCs.

In the cathode (oxygen electrode) of PEMFC, which is operating at around 0.6 to 0.75 V vs. Ag/AgCl (equivalent to 0.4 to 0.55 V vs. SHE) in oxygen-rich condition [14], the adsorbed S species can be spontaneously oxidized. In the anode (hydrogen electrode), in contrast, operatable and efficient mitigation techniques such as heat treatment, ozone addition and utilization of crossover oxygen are necessary to promote the desorption of S species [15] because of its negative operating potential around −0.2 V vs. Ag/AgCl (equivalent to 0.0 V vs. SHE) [15,16].

The adsorption/desorption behavior of S species at Pt single crystal surfaces has been extensively studied at the atomic scale using various surface analysis techniques from the perspective of fundamental surface science [17–21], which recently has also been studied in relation to S poisoning of Pt electrocatalysts in PEMFCs [18,22–24]. These studies revealed that the S species adsorbed on the Pt(111) single crystal surfaces can be removed by oxidative desorption in the potential range more positive than 0.8 V vs. Ag/AgCl [22,23]. We studied the face-orientation dependent oxidative desorption using single crystal Pt (111), Pt(110) and Pt(100) surfaces and found that SO_2 formed by the oxidation of elemental S was easily desorbed from the Pt(111) surface compared to the other surfaces due to the smaller adsorption energy of SO_2 at the Pt(111) surface than that at the other surfaces [25]. In

* Corresponding author at: Research Center for Energy and Environmental Materials (GREEN), National Institute for Materials Science (NIMS), Tsukuba, Ibaraki 305-0044, Japan.
E-mail address: MASUDA.Takuya@nims.go.jp (T. Masuda).

https://doi.org/10.1016/j.elecom.2025.108050
Received 31 July 2025; Received in revised form 11 September 2025; Accepted 19 September 2025
Available online 20 September 2025

addition, from the investigation using the (111) surfaces of single crystals of Pt-based bimetallic alloys, we found that alloying with foreign metal atoms such as Cu, Co and Fe, which have smaller atomic radius than that of Pt, improved the oxidative desorption of S due to the downshift of d-band center [26].

Although oxidative desorption is an effective recovery technique from S poisoning, simultaneous Pt oxide formation and following reduction cause the formation of low-coordinated Pt sites with low stability against dissolution [27,28]. In addition, such very positive potential cannot be applied to the anode because it causes the corrosion of carbon support, leading to the rapid and irreversible degradation of PEMFCs [29]. Thus, an alternative mitigation technique which can accelerate the removal of the adsorbed S species in a milder condition, i.e., in the less positive potential range is strongly desired to avoid the deterioration of catalytic activity during the recovery from the S poisoning.

Ce species are used as promoters to facilitate the oxidative decomposition of adsorbed species on catalyst surfaces through their oxygen storage/supplying capability accompanying with the redox behavior of the CeO_2/Ce_2O_3 [30]. In the present study, we modified a Pt(111) surface with Ce species by being immersed in an aqueous solution saturated with H_2 gas and demonstrated its enhanced oxidative desorption capability for adsorbed S species, over a Ce-free bare Pt(111) surface.

2. Experimental

2.1. Material

The Pt (111) single-crystal disk (99.99 %, diameter:10 mm, thickness: 5 mm) was purchased from Surface Preparation Laboratory. Ultrapure reagent-grade $HClO_4$ (60 %) and reagent-grade Na_2S (98.0 %) purchased from Wako Pure Chemicals, and high purity reagent-grades $Ce(NO_3)_3{\bullet}6H_2O$ purchased from Kanto Chemical were used without further purification. Water was purified using a Milli-Q system (ELGA LabWater). Ultrapure Ar (99.999 %)/H_2 (99.999 %) mixed gases (95:5) were purchased from Suzuki Shokan.

2.2. Sample preparation

Prior to each measurement, the Pt(111) single-crystal disk was annealed using induction heater at 1600 °C for more than 1 h under the flowing Ar and H_2 mixed gas [31]. After cooling under the Ar/H_2 flow for 7 min, the clean Pt(111) disk was immersed in a 0.01 M $Ce(NO_3)_3$ + 0.1 M $HClO_4$ aqueous solution with bubbling Ar/H_2 gas through the solution for 1 h to yield a Pt(111) surface modified with Ce species, denoted as Ce-modified Pt(111) surface or "Ce/Pt(111)". The open circuit potential under this procedure was around −0.2 V vs. Ag/AgCl (equivalent to 0.0 V vs. SHE [32,33]). The Ce-modified Pt(111) surface can be also achieved by holding the potential at −0.2 V vs. Ag/AgCl in the 0.01 M $Ce(NO_3)_3$ + 0.1 M $HClO_4$ aqueous solution, instead of bubbling Ar/H_2 gas through the solution.

The Ce-free and Ce-modified Pt(111) surfaces were immersed in a 1 mM Na_2S aqueous solution under the flow of Ar/H_2 gas for 1 h (referred to as "S/Pt(111)" and "S/Ce/Pt(111)", respectively). After being rinsed with water, those Pt(111) disks were transferred to the electrochemical cell, with keeping a droplet of water on the surface to avoid any surface contamination.

2.3. Electrochemical measurements

Electrochemical measurements were performed at RT using a three-electrode electrochemical cell in the hanging-meniscus configuration. A Ag/AgCl electrode (saturated NaCl, +0.200 V vs. SHE) [32,33], a Pt wire and the Pt(111) surfaces were used as a reference, a counter, and a working electrode, respectively. The potential of the working electrode was controlled by a Potentiostat (Hokuto Denko, HAB-151 A). Potential dependent current response was recorded by a data logger (Graphtec, GL900). Cyclic voltammetry measurements of the Pt(111) surfaces were carried out in a 0.1 M $HClO_4$ aqueous electrolyte solution deaerated by ultrapure Ar gas. Hereafter, the potential was expressed with respect to Ag/AgCl unless otherwise specified throughout the paper.

2.4. X-ray photoelectron spectroscopy (XPS)

XPS measurements were performed using AXIS-NOVA (Shimadzu Kratos) equipped with a monochromatic Al-Kα source at an operating X-ray power of 300 W without charge neutralization. The photoelectron take-off angle was fixed at 90°. The analysis area was a spot with a diameter of 110 μm, and the energy of the photoelectrons passing through the analyzer (pass energy) was 80 eV. The vacuum pressure in the analysis chamber was $\sim 1.5 \times 10^{-8}$ Torr. The position of C 1 s peak at 285.0 eV was used to calibrate the entire spectra and the intensities of Ce 3d, S 2p and O 1 s peaks were normalized by that of C 1 s peak of the same sample.

2.5. X-ray absorption near edge structure (XANES)

XANES measurements were performed at BL9A of the Photon Factory (PF) operated at 2.5 GeV of the High Energy Accelerator Research Organization. XANES spectra at the Ce L_3-edge for reference samples and the Ce-modified Pt(111) surface were recorded in air in a transmission configuration and a polarization dependent total reflection fluorescence configuration [34,35], respectively.

3. Result & discussion

Fig. 1 A shows CVs of Ce-free Pt(111) electrode before and after adsorption of S species, i.e., bare and "S/Pt(111)", in various potential regions. When the potential was swept between −0.20 and 0.50 V for "S/Pt(111)" (Fig. 1 A b), characteristic electrochemical responses of bare Pt(111) electrode such as adsorption/desorption of hydrogen (H-ads/H-des) and hydroxyl species (OH-ads/OH-des) (Fig. 1 A a) completely disappeared due to the adsorption of S, confirming the reduced electrochemically active surface area [25]. S 2p region of XPS spectra of Ce-free "S/Pt(111)" electrode (Fig. 1 C b) showed a pair of peaks corresponding to the adsorbed elemental S, S_{ad}, at 162.8 eV (S $2p_{3/2}$) and 164.0 eV (S $2p_{1/2}$) [18–21]. The potential cycling between −0.20 and 0.50 V (Fig. 1 A b) did not cause any significant change in S 2p region of XPS (Fig. 1 C c). When the positive potential limit was extended up to 0.80 V (Fig. 1 A c), however, oxidation current started to flow from 0.70 V, showing the oxidation of S_{ad} species to SO_2 and/or SO_4^{2-} [25,36]. In the successive reverse scan (Fig. 1 A c), peaks due to the reduction of SO_2 were observed at 0.20 and −0.10 V [25,36]. By repeating this potential cycling between −0.20 V and 0.80 V (Fig. 1 A c), current waves due to hydrogen adsorption/desorption gradually recovered. As shown in Fig. 1 C d, a pair of peaks corresponding to S_{ad} at 162.8 eV decreased significantly, while a small peak appeared at around 167.5 eV, which is assignable to sulfur oxides such as SO_2, SO_3 and SO_4^{2-} [18,25,37]. These results confirm the oxidative desorption of S_{ad} in the potential range more positive than 0.70 V and the (partial) adsorption of oxidatively-formed SO_x, on the surface [25]. In O 1 s region, a peak corresponding to physisorbed species such as ClO_4^- and carboxyl groups in organic contaminations were observed under all the conditions (Fig. 1 D a-d), where Fig. 1 D d may include the component of SO_x.

Fig. 1 E a shows the CVs of the "Ce/Pt(111)" surface measured in a 0.1 M $HClO_4$ aqueous solution. After the immersion of Pt(111) surface in the 0.01 M $Ce(NO_3)_3$ + 0.1 M $HClO_4$ aqueous solution deaerated by Ar/H_2 gas, the characteristic hydrogen adsorption/desorption waves were significantly distorted and the symmetric current waves due to the adsorption/desorption of hydroxyl species were absent, suggesting the modification of Pt(111) surface with Ce species. Comparing the CVs of the bare Pt(111) and "Ce/Pt(111)" (Fig. S1), the charge integration of

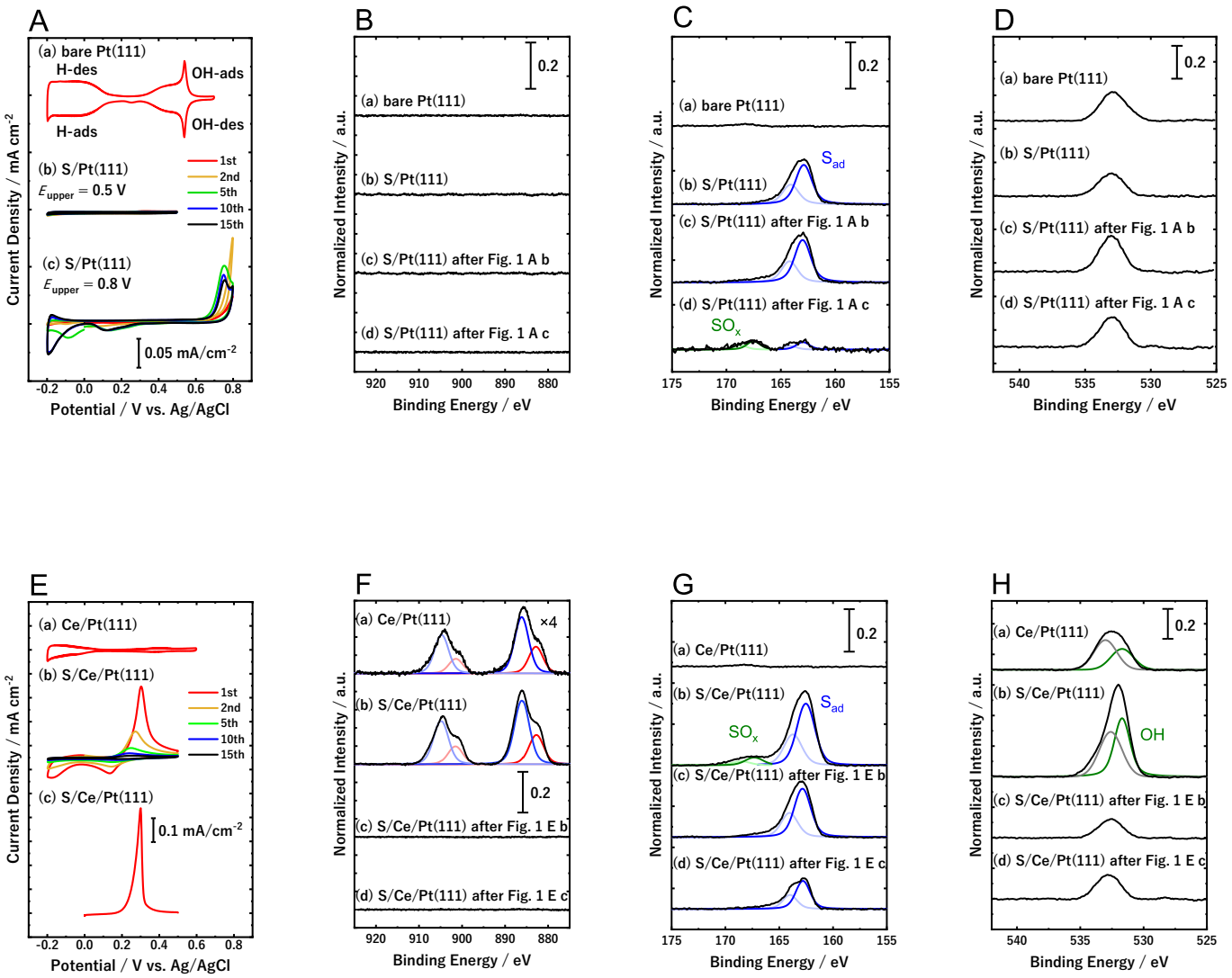

Fig. 1. CVs of (A) the Ce-free and (E) Ce-modified Pt(111) surfaces before and after adsorption of S species, in the various potential regions in 0.1 M $HClO_4$ aqueous solution with a scan rate of 50 mV s^{-1}. Photoelectron spectra in the regions of (B, F) Ce 3d, (C, G) S 2p and (D, H) O 1 s observed for (B—D) the Ce-free and (F—H) Ce-modified Pt(111) surfaces, in which spectra (a) and (b) were obtained before and after being immersed in a 1 mM Na_2S aqueous solution, respectively, and spectra (c) and (d) were obtained after recording the voltammograms (b) and (c), respectively.

hydrogen desorption current at the "Ce/Pt(111)" surface was found to be 39 % of that at the Ce-free bare Pt(111) surface, showing that 61 % of the hydrogen adsorption site was covered by Ce species.

Decrease in hydrogen adsorption/desorption waves was also observed in CV of polycrystalline Pt surface after the immersion in the $Ce(NO_3)_3$ aqueous solution saturated with Ar/H_2 gas (Fig. S2 (a)) or holding the electrode potential at −0.2 V vs. Ag/AgCl (Fig. S2 (b)), implying that polycrystalline Pt surface can be modified with Ce species. However, CV of polycrystalline Pt surface remained unchanged after being immersed in the aqueous solution of $Ce(NO_3)_3$ without Ar/H_2 gas bubbling (Fig. S2 (c)). Moreover, CVs of polycrystalline Pt surface before and after drop-casting the aqueous solution of $Ce(NO_3)_3$ (Fig. S2 (d)) are identical to each other. These results suggest that the physisorbed Ce species, probably Ce^{3+} ions, can be easily desorbed from the Pt surface and that either Ar/H_2 bubbling or keeping the potential at −0.2 V is essential to modify the Pt surface with insoluble Ce species such as hydroxide. It is noted that, in the cathodic electrolytic deposition of cerium oxide (ceria, CeO_2) [38–41], the generation of hydroxide ions (OH^-) by the reduction of species such as water, nitrate, and dissolved oxygen increases the local pH in the vicinity of electrode surface, which leads to the formation of cerium hydroxide $Ce(OH)_3$ as an intermediate and finally to the deposition of CeO_2 films due to further oxidation of the hydroxide [40,41]. In our case, under Ar/H_2 gas bubbling or applying −0.2 V, the $Ce(OH)_3$ precipitate or layer is probably produced by an increase in the local pH at the interface, while the oxidation to CeO_2 do not occur, considering from the *E*–pH diagram for the Ce–$HClO_4$–H_2O system [42].

The Ce 3d region of XPS spectra of the Ce-modified Pt(111) electrodes before and after the immersion in Na_2S solution, i.e., "Ce/Pt (111)" and "S/Ce/Pt(111)", confirmed the presence of Ce(III) species on the Pt(111) surface (Fig. 1 F a and b, respectively) [42–45]; in more detail, the four noticeable peaks observed are characteristic of Ce(III) oxidation state and can be deconvoluted into two doublets, one at ~887 and ~905 eV assignable to $3d^94f^1$ final state, and the other at ~883 and ~901 eV often assigned to $3d^94f^2$ final state [46,47]. Photoelectron spectrum in the O 1 s region of the "Ce/Pt(111)" and "S/Ce/Pt(111)" surfaces without electrochemical treatment (Fig. 1 H a and b, respectively) clearly showed the peak at 531.8 eV corresponding to Ce hydroxide [44,45], in addition to the peak at 532.7 eV from physisorbed ClO_4^-, carboxyl groups in organic contaminations and the component associated with SO_x observed also for Ce-free surface (Fig. 1 D). It is noted that there was no component at ~530 eV corresponding to lattice

oxygen in CeO_2 [44,45], suggesting the absence of Ce(IV) species. Ce L_3-edge XANES spectrum of the Ce-modified Pt(111) electrode (Fig. 2 a) showed a single peak characteristic to Ce(III) species at 5724 eV [48], showing that Ce species deposited on at Pt(111) surface is Ce(III) state, presumably, $Ce(OH)_3$. It is worth noting that, although a surface-sensitive total reflection configuration was adopted, the amount of Ce species is at the sub-monolayer level. Additionally, absorption and scattering in air have attenuated the signal, resulting in spectra with significant noise.

For the "S/Ce/Pt(111)" specimen, the peaks corresponding to S_{ad} were observed at 162.5 eV (S $2p_{3/2}$) and 163.7 eV (S $2p_{1/2}$) in S 2p region of XPS spectra (Fig. 1 G b), of which binding energies were slightly lower than, but almost the same as, those for Ce-free "S/Pt(111)" specimen (Fig. 1 C b). Interestingly, a large oxidation peak and coupled reduction peak appeared at around 0.32 and 0.18 V, respectively, in CV of "S/Ce/Pt(111)" electrode (Fig. 1 E b), whereas no current peaks were observed for the Ce-free "S/Pt(111)" electrode scanned in the same potential region (Fig. 1 A b). As described above, the cathodic current wave which we previously attributed to the reduction of SO_2 to S_{ad} [25] was observed between 0.20 and −0.10 V in the CV of the Ce-free "S/Pt (111)" electrode after sweeping the potential up to 0.8 V to oxidize S_{ad} (Fig. 1 A c). Thus, a pair of oxidation (at 0.32 V) and reduction (at 0.18 V) peaks (Fig. 1 E b) can be attributed to the oxidation of S_{ad} and reduction of SO_2, respectively. The charge integration of this oxidation peak was estimated to be 360 μC cm^{-2}, which was in reasonable agreement with the theoretical charge density of 322 μC cm^{-2} for the four-electron oxidation of S_{ad} in the $(\sqrt{3} \times \sqrt{3})$-R30° structure on the Pt (111) to SO_2 [25].

With the number of potential cycling between −0.20 V and 0.50 V, the oxidation peak gradually shifted to the less positive potential and both oxidation and reduction peaks became smaller (Fig. 1 E b). After the 15th potential cycling (Fig. 1 E b), the S 2p peaks due to S_{ad} at 162.8 eV decreased to 80 % (Fig. 1 G c), simultaneously with the disappearance of Ce 3d peaks (Fig. 1 F c) and O 1 s component associated with hydroxide (Fig. 1 H c), suggesting the desorption of insoluble Ce species, presumably $Ce(OH)_3$, from the surface of "S/Ce/Pt(111)" specimen together with the oxidative desorption of S_{ad}.

When the "S/Ce/Pt(111)" electrode was removed from the electrolyte solution while keeping the potential at 0.5 V following the anodic (positive going) single scan from 0.0 V (Fig. 1 E c), the normalized peak area of S 2p decreased to 25 % in the photoelectron spectra (Fig. 1 G d). Previously, we proposed that the oxidatively formed SO_2 can be desorbed from the surface or reduced to be S_{ad}, and desorption of SO_2 from Pt surfaces is the key process that significantly affects the overall recovery rate from S poisoning [25]. In the present study, the oxidative desorption of S_{ad} was also accelerated by skipping the successive cathodic (negative going) scan due to the lack of regeneration of S_{ad} from SO_2.

Considering that the current peak due to the oxidation of S_{ad} to SO_2 was observed at 0.84 V at a Ce-free Pt(111) surface [25], the Ce modification enables the oxidation of S_{ad} at ~0.5 V less positive potential. Cerium oxide is used as a co-catalyst for three-way catalysts to eliminate the toxic exhaust gases from automobiles, due to its excellent oxygen storage capability; lattice oxygen can be donated to promote the oxidation reaction of toxic gases such as carbon monoxide (CO) [49]. Similar bifunctional mechanism accelerating the oxidative desorption of CO was also reported in electrocatalytic oxidation of CO adsorbed on Pt—Ru alloy surface [50]. In the present case, oxygen species such as OH trapped within the adsorbed Ce species can be used as an oxygen source to promote the oxidation of S_{ad} at the Ce-modified Pt(111) surface and the resulting ionic Ce(III) species dissolved in the electrolyte solution as shown in Fig. 3.

4. Conclusion

The oxidative desorption of S_{ad} was significantly promoted by modifying the Pt(111) surface with Ce species; oxidation of S_{ad} occurred at 0.32 V at the Ce-modified Pt(111) surface whereas 0.84 V at the Ce-free Pt(111) surface. During this promotive effect on the oxidative desorption, not only a part of S_{ad} but also Ce species desorbed from the surface, suggesting that the Ce species act as a sacrificial substance. Ce species are often added in the anode of PEMFCs as a radical quencher [51–53]. In addition, the modification of Pt surface with Ce species can be achieved by being exposed to H_2 environment or keeping the potential at −0.2 V vs. Ag/AgCl (equivalent to 0 V vs. SHE) which is similar to the practical operation condition of the PEMFC anode. Thus, the cycle consisting of the Pt modification with Ce species and Ce-involved oxidative desorption of S_{ad} can be a practical mitigation technique against the S poisoning using a small amount of cross-over oxygen from the cathode.

CRediT authorship contribution statement

Tetsuro Morooka: Writing – original draft, Methodology, Investigation, Formal analysis, Data curation, Conceptualization. **Tamao Shishido:** Methodology. **Takuya Nakanishi:** Writing – review & editing, Validation, Investigation, Formal analysis. **Takuya Masuda:**

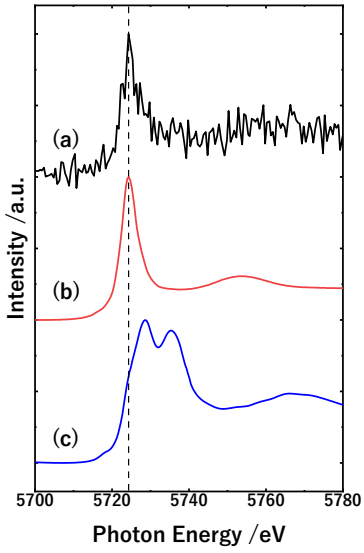

Fig. 2. XANES spectrum at the Ce L_3-edge for the Ce-modified Pt(111) electrode (a) together with reference spectra for $Ce(NO_3)_3$ (b) and CeO_2 powder (c).

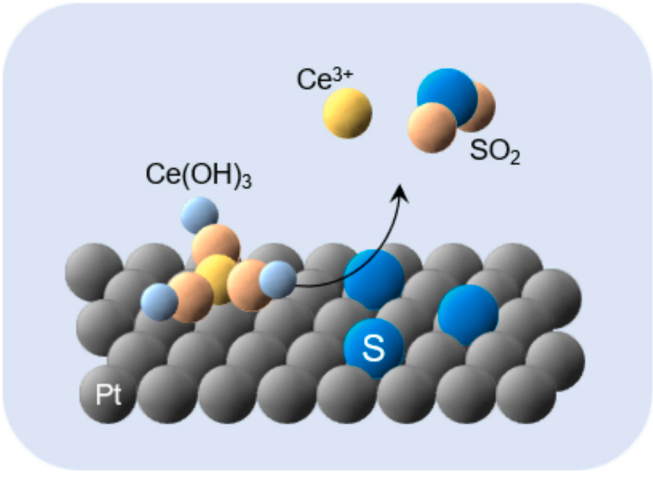

Fig. 3. Schematic illustration of the promoted oxidative desorption of S_{ad} at the Ce-modified Pt(111) surface.

Writing – review & editing, Validation, Supervision, Resources, Project administration, Investigation, Funding acquisition, Formal analysis, Conceptualization.

Declaration of competing interest

The authors declare the following financial interests/personal relationships which may be considered as potential competing interests: Takuya Masuda reports financial support was provided by New Energy and Industrial Technology Development Organization. If there are other authors, they declare that they have no known competing financial interests or personal relationships that could have appeared to influence the work reported in this paper.

Acknowledgement

This paper is based on results obtained from a project, JPNP20003, commissioned by the New Energy and Industrial Technology Development Organization (NEDO).

Appendix A. Supplementary data

Supplementary data to this article can be found online at https://doi.org/10.1016/j.elecom.2025.108050.

Data availability

Data will be made available on request.

References

[1] K. Kodama, T. Nagai, A. Kuwaki, R. Jinnouchi, Y. Morimoto, Challenges in applying highly active Pt-based nanostructured catalysts for oxygen reduction reactions to fuel cell vehicles, Nat. Nanotech. 16 (2021) 140–147, https://doi.org/10.1038/s41565-020-00824-w.

[2] M. Shao, Q. Chang, J.-P. Dodelet, R. Chenitz, Recent advances in Electrocatalysts for oxygen reduction reaction, Chem. Rev. 116 (2016) 3594–3657, https://doi.org/10.1021/acs.chemrev.5b00462.

[3] H. Xu, Y. Liu, K. Wang, L. Jin, J. Chen, H. Chen, G. He, High-entropy layered double hydroxides tailor Pt electron state for promoting acidic hydrogen evolution reaction, J. Colloid Interface Sci. 684 (2025) 566–574, https://doi.org/10.1016/j.jcis.2025.01.077.

[4] X. Chu, K. Wang, W. Qian, H. Xu, Surface and interfacial engineering of 1D Pt-group nanostructures for catalysis, CoordinationChemistryReviews 477 (2023) 214952, https://doi.org/10.1016/j.ccr.2022.214952.

[5] R. Borup, J. Meyers, B. Pivovar, Y.S. Kim, R. Mukundan, N. Garland, D. Myers, M. Wilson, F. Garzon, D. Wood, P. Zelenay, K. More, K. Stroh, T. Zawodzinski, J. Boncella, J.E. McGrath, M. Inaba, K. Miyatake, M. Hori, K. Ota, Z. Ogumi, S. Miyata, A. Nishikata, Z. Siroma, Y. Uchimoto, K. Yasuda, K.-I. Kimijima, N. Iwashita, Scientific aspects of polymer electrolyte fuel cell durability and degradation, Chem. Rev. 107 (2007) 3904–3951, https://doi.org/10.1021/cr050182l.

[6] M.K. Debe, Electrocatalyst approaches and challenges for automotive fuel cells, Nature 486 (2012) 43–51, https://doi.org/10.1038/nature11115.

[7] F. Garzon, T. Lopes, T. Rockward, J.-M. Sansiñena, B. Kienitz, R. Mukundan, The impact of impurities on long-term PEMFC performance, ECS Trans. 25 (2009) 1575–1583, https://doi.org/10.1149/1.3210713.

[8] W. Dong, C. Xu, W. Zhao, M. Xin, Y. Xiang, A. Zheng, M. Dou, S. Ke, J. Dong, L. Qiu, G. Xu, Poisoning effects of H_2S, CS_2, and COS on hydrogen oxidation reaction over Pt/C catalysts, ACS Appl Energy Mater 5 (2022) 12640–12650, https://doi.org/10.1021/acsaem.2c02284.

[9] T.V. Reshetenko, Impacts of operating conditions on the recovery of proton exchange membrane fuel cells exposed to sulfur dioxide in an air stream, J. Power Sources 559 (2023) 232676, https://doi.org/10.1016/j.jpowsour.2023.232676.

[10] R. Mohtadi, W.-K. Lee, S. Cowan, J.W. Van Zee, M. Murthy, Effects of hydrogen sulfide on the performance of a PEMFC, Electrochem. Solid St. 6 (2003) A272–A274, https://doi.org/10.1149/1.1621831.

[11] S. Ke, L. Qiu, W. Zhao, C. Sun, B. Cui, G. Xu, M. Dou, Understanding of correlation between electronic properties and sulfur tolerance of Pt-based catalysts for hydrogen oxidation, ACS Appl. Mater. Interfaces 14 (2022) 7768–7778, https://doi.org/10.1021/acsami.1c18905.

[12] R. Mohtadi, W.K. Lee, J.W. Van Zee, The effect of temperature on the adsorption rate of hydrogen sulfide on Pt anodes in a PEMFC, Appl. Cat. B: Environ. 56 (2005) 37–42, https://doi.org/10.1016/j.apcatb.2004.08.012.

[13] W. Shi, B. Yi, M. Hou, F. Jing, P. Ming, Hydrogen sulfide poisoning and recovery of PEMFC Pt-anodes, J. Power Sources 165 (2007) 814–818, https://doi.org/10.1016/j.jpowsour.2006.12.052.

[14] A.Z. Weber, R.L. Borup, R.M. Darling, P.K. Das, T.J. Dursch, W. Gu, D. Harvey, A. Kusoglu, S. Litster, M.M. Mench, R. Mukundan, J.P. Owejan, J.G. Pharoah, M. Secanell, I.V. Zenyuk, A critical review of modeling transport phenomena in polymer-electrolyte fuel cells, J. Electrochem. Soc. 161 (2014) F1254–F1299, https://doi.org/10.1149/2.0751412jes.

[15] S. Ke, C. Sun, B. Cui, Y. Qin, M. Dou, Operatable and efficient mitigation strategies for H_2S poisoning in proton exchange membrane fuel cells: releasing Pt reactive sites for hydrogen oxidation, ACS Appl Energy Mater 6 (2023) 3337–3346, https://doi.org/10.1021/acsaem.2c04026.

[16] B.K. Kakati, A.R.J. Kucernak, Gas phase recovery of hydrogen sulfide contaminated polymer electrolyte membrane fuel cells, J. Power Sources 252 (2014) 317–326, https://doi.org/10.1016/j.jpowsour.2013.11.077.

[17] N. Batina, J.W. McCargar, L. Laguren-Davidson, C.-H. Lin, A.T. Hubbard, Structure and composition of platinum(111) and platinum(100) surfaces as a function of electrode potential in aqueous sulfide solutions, Langmuir 5 (1989) 123–128, https://doi.org/10.1021/la00085a022.

[18] C.-H. Chen, A. Halford, M. Walker, C. Brennan, S.C.S. Lai, D.J. Fermin, P.R. Unwin, P. Rodriguez, Electrochemical characterization and regeneration of sulfur poisoned Pt catalysts in aqueous media, J. Electroanal. Chem. 816 (2018) 138–148, https://doi.org/10.1016/j.jelechem.2018.03.015.

[19] J.A. Rodriguez, M. Kuhn, J. Hrbek, The bonding of sulfur to a Pt(111) surface: photoemission and molecular orbital studies, Chem. Phys. Lett. 251 (1996) 13–19, https://doi.org/10.1016/0009-2614(96)00066-8.

[20] Z. Yang, R. Wu, J.A. Rodriguez, First-principles study of the adsorption of sulfur on Pt(111): S core-level shifts and the nature of the Pt-S bond, Phys. Rev. B 65 (2002) 155409, https://doi.org/10.1103/physrevb.65.155409.

[21] J.A. Rodriguez, J. Dvorak, T. Jirsak, G. Liu, J. Hrbek, Y. Aray, C. González, Coverage effects and the nature of the metal−sulfur bond in S/au(111): high-resolution photoemission and density-functional studies, J. Am. Chem. Soc. 125 (2003) 276–285, https://doi.org/10.1021/ja021007e.

[22] Y.-E. Sung, W. Chrzanowski, A. Zolfaghari, G. Jerkiewicz, A. Wieckowski, Structure of chemisorbed sulfur on a Pt(111) electrode, J. Am. Chem. Soc. 119 (1997) 194–200, https://doi.org/10.1021/ja962637h.

[23] Y.E. Sung, W. Chrzanowski, A. Wieckowski, A. Zolfaghari, S. Blais, G. Jerkiewicz, Coverage evolution of sulfur on Pt(111) electrodes: from compressed overlayers to well-defined islands, Electrochim. Acta 44 (1998) 1019–1030, https://doi.org/10.1016/S0013-4686(98)00206-0.

[24] L. Kattwinkel, O.M. Magnussen, Optical reflectance studies on the oxidation of chemisorbed sulfur at the Pt(111) electrode, Electrochim. Acta 434 (2022) 141297, https://doi.org/10.1016/j.electacta.2022.141297.

[25] T. Morooka, T. Shishido, R. Derivaraprasad, G. Elumalai, M. Aoki, T. Shirasawa, T. Nakanishi, A. Ishikawa, T. Kondo, T. Masuda, Potential-dependent and face orientation-dependent electrochemical oxidative desorption behavior of sulfur species adsorbed on platinum single-crystal surfaces, J. Phys. Chem. C 128 (2024) 16426–16436, https://doi.org/10.1021/acs.jpcc.4c03227.

[26] M. Aoki, T. Shishido, T. Morooka, T. Nakanishi, T. Masuda, Electrochemical oxidative desorption of adsorbed sulfur species on (111) surfaces of single crystals of pure Pt and Pt-based bimetallic alloys, J. Phys. Chem. C 129 (2025) 2122–2131, https://doi.org/10.1021/acs.jpcc.4c06652.

[27] F. Sonsudin, T. Masuda, K. Ikeda, H. Naohara, K. Uosaki, Effect of coating by Perfluorosulfonated ionomer film on electrochemical behaviors of Pt(111) electrode in acidic solutions, Chem. Lett. 39 (2010) 286–287, https://doi.org/10.1246/cl.2010.286.

[28] P.P. Lopes, D. Strmcnik, D. Tripkovic, J.G. Connell, V. Stamenkovic, N. M. Markovic, Relationships between atomic level surface structure and stability/activity of platinum surface atoms in aqueous environments, ACS Catal. 6 (2016) 2536–2544, https://doi.org/10.1021/acscatal.5b02920.

[29] O. Kim, S.J. Yoo, J.Y. Kim, S.K. Cho, H.S. Park, S.Y. Lee, B. Seo, J.H. Jang, K. H. Lim, H.-Y. Park, Impact of fuel starvation–induced anode carbon corrosion in proton exchange membrane fuel cells on the structure of the membrane electrode assembly and exhaust gas emissions: a quantitative case study, J. Power Sources 615 (2024) 235032, https://doi.org/10.1016/j.jpowsour.2024.235032.

[30] J. Kašpar, P. Fornasiero, M. Graziani, Use of CeO2-based oxides in the three-way catalysis, Catal. Today 50 (1999) 285–298, https://doi.org/10.1016/S0920-5861(98)00510-0.

[31] T. Masuda, H. Fukumitsu, T. Kondo, H. Naohara, K. Tamura, O. Sakata, K. Uosaki, Structure of Pt(111)/ionomer membrane Interface and its Bias-induced change in membrane electrode assembly, J. Phys. Chem. C 117 (2013) 12168–12171, https://doi.org/10.1021/jp402251z.

[32] A. Shatkay, A. Lerman, Individual activities of sodium and chloride ions in aqueous solutions of sodium chloride, Anal. Chem. 41 (1969) 514–517, https://doi.org/10.1021/ac60272a006.

[33] H.R. Rabie, G. Wilczek-Vera, J.H. Vera, Activities of individual ions from infinite dilution to saturated solutions, J. Solution Chem. 28 (1999) 885–913, https://doi.org/10.1023/A:1021736315580.

[34] W.-J. Chun, K. Asakura, Y. Iwasawa, Polarization-dependent Total-reflection fluorescence XAFS study of Mo oxides on a rutile TiO2(110) single crystal surface, J. Phys. Chem. B 102 (1998) 9006–9014, https://doi.org/10.1021/jp9820368.

[35] T. Masuda, Y. Sun, H. Fukumitsu, H. Uehara, S. Takakusagi, W.-J. Chun, T. Kondo, K. Asakura, K. Uosaki, Various active metal species incorporated within molecular layers on Si(111) electrodes for hydrogen evolution and CO2 reduction reactions, J. Phys. Chem. C 120 (2016) 16200–16210, https://doi.org/10.1021/acs.jpcc.6b00895.

[36] C. Quijada, J.L. Vázquez, J.M. Pérez, A. Aldaz, Voltammetric behaviour of irreversibly adsorbed SO_2 on a Pt(111) electrode in sulphuric acid medium,

J. Electroanal. Chem. 372 (1994) 243–250, https://doi.org/10.1016/0022-0728(93)03261-M.
[37] R. Streber, C. Papp, M.P.A. Lorenz, O. Hofet, W. Zhao, S. Wickert, E. Darlatt, A. Bayer, R. Denecke, H.P. Steinrueck, Influence of steps on the adsorption and thermal evolution of SO_2 on clean and oxygen precovered Pt surfaces, J. Phys. Chem. C 114 (2010) 19734–19743, https://doi.org/10.1021/jp105994f.
[38] Y. Zhou, J.A. Switzer, Growth of cerium(IV) oxide films by the electrochemical generation of base method, J. Alloys Compd. 237 (1996) 1–5, https://doi.org/10.1016/0925-8388(95)02048-9.
[39] I. Zhitomirsky, A. Petric, Electrolytic and electrophoretic deposition of CeO_2 films, Mater. Lett. 40 (1999) 263–268, https://doi.org/10.1016/S0167-577X(99)00087-7.
[40] L. Arurault, P. Monsang, J. Salley, R.S. Bes, Electrochemical preparation of adherent ceria coatings on ferritic stainless steel, Thin Solid Films 466 (2004) 75–80, https://doi.org/10.1016/j.tsf.2004.02.039.
[41] Y. Hamlaoui, F. Pedraza, L. Tifouti, Investigation of electrodeposited cerium oxide based films on carbon steel and of the induced formation of carbonated green rusts, Corros. Sci. 50 (2008) 2182–2188, https://doi.org/10.1016/j.corsci.2008.05.017.
[42] S.A. Hayes, P. Yu, T.J. O'Keefe, M.J. O'Keefe, J.O. Stoffer, The phase stability of cerium species in aqueous systems : I. E-pH diagram for the system, J. Electrochem. Soc. 149 (2002) C623–C630, https://doi.org/10.1149/1.1516775.
[43] K. Fugane, T. Mori, D.R. Ou, P. Yan, F. Ye, H. Yoshikawa, J. Drennan, Improvement of cathode performance on Pt-CeO_x by optimization of electrochemical pretreatment condition for PEFC application, Langmuir 28 (2012) 16692–16700, https://doi.org/10.1021/la302912r.
[44] N. Mora, E. Cano, J. Polo, J. Puente, J. Bastidas, Corrosion protection properties of cerium layers formed on tinplate, Corros. Sci. 46 (2004) 563–578, https://doi.org/10.1016/S0010-938X(03)00171-9.
[45] L. Martinez, E. Roman, J.L. de Segovia, S. Poupard, J. Creus, F. Pedraza, Surface study of cerium oxide based coatings obtained by cathodic electrodeposition on zinc, Appl. Surf. Sci. 257 (2011) 6202–6207, https://doi.org/10.1016/j.apsusc.2011.02.033.
[46] A. Pfau, K.D. Schierbaum, The electronic structure of stoichiometric and reduced CeO2 surfaces: an XPS, UPS and HREELS study, Surf. Sci. 6028 (1994) 71–80, https://doi.org/10.1016/0039-6028(94)90027-2.
[47] D.A. Creaser, P.G. Harrison, M.A. Morris, B.A. Wolfindale, X-ray photoelectron spectroscopic study of the oxidation and reduction of a cerium(III) oxide/cerium foil substrate, Catal. Lett. 23 (1994) 13–24, https://doi.org/10.1007/BF00812127.
[48] T. Masuda, H. Fukumitsu, K. Fugane, H. Togasaki, D. Matsumura, K. Tamura, Y. Nishihata, H. Yoshikawa, K. Kobayashi, T. Mori, K. Uosaki, Role of cerium oxide in the enhancement of activity for the oxygen reduction reaction at Pt–CeO_x nanocomposite Electrocatalyst - an in situ electrochemical X-ray absorption fine structure study, J. Phys. Chem. C 116 (2012) 10098–10102, https://doi.org/10.1021/jp301509.
[49] R. Lin, C. Cao, H. Zhang, H. Huang, J. Ma, Electro-catalytic activity of enhanced CO tolerant cerium-promoted Pt/C catalyst for PEM fuel cell anode, Int. J. Hydrogen Energy 37 (2012) 4648–4656, https://doi.org/10.1016/j.ijhydene.2011.05.021.
[50] M. Watanabe, Y.M. Zhu, H. Igarashi, H. Uchida, Mechanism of CO tolerance at Pt-alloy anode catalysts for polymer electrolyte fuel cells, Electrochemistry 68 (2000) 244–251, https://doi.org/10.5796/electrochemistry.68.244.
[51] P. Trogadas, J. Parrondo, V. Ramani, Degradation mitigation in polymer electrolyte membranes using cerium oxide as a regenerative free-radical scavenger, Electrochem. Solid St. 11 (2008) B113–B116, https://doi.org/10.1149/1.2916443.
[52] C. Walkey, S. Das, S. Seal, J. Erlichman, K. Heckman, L. Ghibelli, E. Traversa, J. F. McGinnis, W.T. Self, Catalytic properties and biomedical applications of cerium oxide nanoparticles, environ, Sci.: Nano 2 (2015) 33–53, https://doi.org/10.1039/c4en00138a.
[53] Z. Rui, J. Liu, Understanding of free radical scavengers used in highly durable proton exchange membranes, Prog. Nat. Sci.: Mater. Int. 30 (2020) 732–742, https://doi.org/10.1016/j.pnsc.2020.08.013.